Journal of Materials Chemistry A

Accepted Manuscript

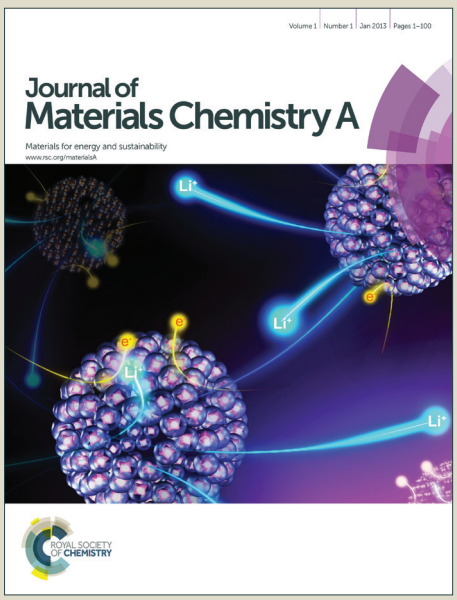

ROYAL SOCIETY OF CHEMISTRY

www.rsc.org/materialsA

Improved power output by polyvinyl alcohol in the anode of microbial fuel cell

X. F. Chen[a], X. S. Wang[a], K. T. Liao[a], L. Z. Zeng[c], L. D. Xing [a,b], X. W. Zhou[a], X. W. Zheng[a], W. S. Li [a,b*]

In this study, polyvinyl alcohol (PVA) is proposed as a new binder to improve power output of microbial fuel cell. The physical and chemical properties of PVA are characterized with Fourier transform infrared spectroscopy (FTIR), thermogravimetric analyzer (TGA), contact angle test, density functional theory calculation, and scanning electron microscopy (SEM). The electrochemical performances of the anode using carbon nanotubes as electrocatalyst and PVA as binder are evaluated in a *Escherichia coli* based fuel cell by chronoamperometry, electrochemical impedance spectroscopy (EIS), and polarization curve measurement, with a comparison of the conventional binder, polytetrafluoroethylene (PTFE). It is found that PVA is more hydrophilic and has stronger interaction with the bacterium membrane than PTFE. Accordingly, the anode with PVA as binder facilitates the formation of biofilm and thus exhibits improved electron transfer kinetics between bacteria and anode of microbial fuel cell compared to the anode using PTFE. The MFC using PVA produces the largest maximum output power, 1.631 $W \cdot m^{-2}$, which is 97.9% greater than the largest one produced by the MFC using PTFE (0.824 $W \cdot m^{-2}$).

1. Introduction

Microbial fuel cell (MFC) is a novel electrochemical device which can convert chemical energy into electrical energy by the catalytic activity of microorganisms.[1] MFC has been drawing a rapidly growing research attention because it shows a great potential in energy recovery from wastewater treatment, marine sediment and human excrement in space.[2] The power output of MFC, however, needs to be enhanced for large-scale application.

MFC consists of anode accepting electrons liberated from the bacterium metabolism, cathode delivering the electrons for the oxygen reduction and electrolyte providing ionic transportation path. Many factors affect the power output of MFC, including microbial inoculums, chemical substrate, electron transfer kinetics on anodic and cathode, and electrolyte resistance.[3-4] Among these factors, anodic electron transfer kinetics is the most important because it happens to base on the biofilm, which is difficult to form on anode.[5-7] In the absence of exogenous electron mediators, current production mainly depends on the biofilm. There are two mechanisms involved in the electron transfer between anode and bacteria:[4,8-11] direct electron transfer via microbial wall (path A of Fig. 1) and long-range electron transfer via microbial nanowires (path B of Fig. 1).[12] Accordingly, the electronic conductivity and the biocompatibility of the anode (the formation of a biofilm) are important for bacteria to generate electricity. Therefore, developing an anode that facilitates the formation of biofilm is necessary for improving the power output of MFC.

Various anode electrocatalysts have been reported to be effective for improving power output of MFC, such as carbon nanotubes,[2,13,14] MWCNTs/SnO_2,[15] polyaniline composite,[10,16-18] ZnO/Au,[19] Mo_2C composite.[1,7,20] These studies are mainly focused on the improvement in electronic conductivity of the anode. On the other hand, the surface morphology of anode electrocatalysts has been found to be vital for the formation of biofilm and thus affects significantly the power output of MFC.[21-23] In all these applications, binder is needed but less attention has been paid to its influence on the electrochemical performance of anode.

Binder provides anode with integrity and is thus required to possess good cohesion with anodic electrocatalysts. Poly(tetrafluoroethylene) (PTFE) is the most used binder for battery materials and has been found to be effective for MFC use due to its strong cohesion with anodic electrocatalyst.[24,25] As

shown in Fig. 1, binder exists inevitably on the interface between anode and electrolyte. The electrolyte used for MFC is an aqueous solution. Therefore, a binder with good hydrophilicity is beneficial for the formation of biofilm and thus facilitates the electron transfer between anode and bacteria. Since PTFE is hydrophobic, it can be expected that finding alternatives to PTFE is one of effective approaches for the improvement in power output of MFCs.

Polyvinyl alcohol (PVA) is hydrophilic because it has oxygen-containing groups and has been widely used as emulsifiers and dispersants. PVA is also used in tissue engineering, drug delivery and scaffold for bacterium growth, because it is one kind of polysaccharides with good biocompatibility and good strength.[26-29] Recently, PVA has been successfully used to improve the performance of electrochemical active surface area and adsorption properties.[30,31]

In this study, PVA was proposed as anode binder for MFC for the first time. Its hydrophilicity and biocompatibility were understood and its performance as binder was compared with that of PTFE in MFC based on carbon nanotubes anode with *Escherichia coli* (*E. coil*).

2. Experimental

2.1 Anode preparation

Polyvinyl alcohol (PVA, Aladdin, China) was dissolved in deionized water (DI-water), followed by mixing for 2 hour by magnetic stirring at 60□. The required amount of carbon nanotubes (2 mg/cm^2, CNTs, Chengdu Organic Chemical Co. Ltd., China) was added in the solutions with different contents of PVA (in weight percentage based on CNTs), and then dispersed uniformly under sonication for 30 min. The resulting mixture was coated on carbon felt (3.0 cm × 3.0 cm, Beijing Carbonsci Tech. Co. Ltd) to prepare the anode as described in our previous work.[22] For a comparison, the anode with PTFE as binder was also prepared.

CNTs were used in this work, because CNTs can provide better electronically conductive network with their linear tubes than other carbon materials, which is important for the power output of MFC. Fig. S1 compares the power output of the MFC using carbon nanotubes, activated carbon (AC) and carbon black (CB) as anode electrocatalysts under the same condition (10% PVA). It can be seen from Fig. S1 that the MFC using CNTs exhibits better performance than those using AC and CB.

2.2 Bacterial cultivation

The standard Luria-Bertani medium, containing 10 g peptone, 5 g yeast extract and 10 g sodium chloride per liter DI-water, was used to cultivate *E. coli* (DH5α) at 37 □ for 14 hour. Then the bacterial culture in stationary phase was harvested by centrifugation at 4 □ (6000 rpm, 5 min), and then suspended in 50 mM phosphate-buffered basal medium (PBBM, pH 7.0,) solution containing 2 g L^{-1} glucose.[6] To evaluate the effectiveness of PVA on the MFC based on other bacteria, the performances of MFCs inoculated with the supernatant of an acclimated sludge from a methane-generating pond were also determined.

2.3 MFC construction

Cubic single-chamber MFC was used, as shown in Fig. S2, which consists of a polymethyl methacrylate chamber (5.0 cm×4.0 cm×5.0 cm) and a membrane cathode assemble (MCA, 6.0 cm×6.0 cm). The MCA was prepared with carbon cloth as support and 20% Pt/C as catalyst, which were hot-pressed on one side of a cation exchange membrane (CEM). The cathode catalyst was pasted on the carbon paper with 0.2 mg cm^{-2} Pt/C in a mixture of polyvinylidene fluorine (PVDF) by a weight ratio of 65:15 in 0.8 mL N-methyl-2-pyrrolidone (NMP) as description in our previous report.[22]

The phosphate-buffered basal medium (PBBM) consisting of (per liter of deionized water) 5.8 g NaCl, 0.1 g KCl, 0.25 g NH_4Cl, 10 mL vitamin solution, 10 mL trace mineral solution, and phosphate buffer (50 mM, pH 7.0), was added into anode chamber with 2 g L^{-1} glucose as electron donor. All media for MFC were sterilized by autoclaves (DSX-280B, China) at 126□, 30 min before use. To initiate the MFC experiment, the single chamber was inoculated with 10 mL cell suspension and PBBM in a constant temperature incubator (at 37 □, HPG-280H, China),

as described in our previous report.[7]

2.4 Measurement and Calculation

Electrochemical measurements, including power output, chronoamperometry and electrochemical impedance spectroscopy, were performed on Solartron 1480 potentiostatic (England) in MFC with three electrodes: the carbon felt anode as working electrode, air cathode as counter electrode and Ag/AgCl (saturated with KCl) as reference electrode. Power outputs were obtained by linear sweep voltammetry (scan rate 1 mV s^{-1}) from the open circuit potential to 0 V and constant resistance, in which an external resistor (REX) varying from 50 Ω to 5000 Ω was monitored by a 16-channel voltage collection instrument (AD 8223, China). Before the measurement, the cell was kept quiescent for three days until a constant voltage output was achieved. Power density was calculated according to P = IU/A, in which I is the current, U is the voltage between the working electrode and air cathode and A is the apparent area of the working electrode (9.0 cm^2).[32] Electrochemical impedance spectroscopy was performed in a frequency range of 10^5-0.01Hz with the amplitude of 5mV.

The surface morphologies of anodes were observed by the scanning electron microscopy (SEM, JSM-6510, Japan). Hydrophilicity was determined using contact angle by a contact angle system (JC2000C, China). 10 μL deionized water was dropped on the resulting films, which were prepared by coating binder mixture on a horizontal glass slide and then drying on 60°C. The molecular structure of binders was characterized by Fourier transform infrared (FTIR, BRUKER TENSOR 27, Germany) spectroscopy in the range of 450-4000 cm^{-1}. The thermal stability of binders was analyzed with thermogravimetric analyzer (TGA, Perkine-Elmer TGA7).

All calculations were performed using the Gaussian 09 package.[33] The equilibrium structures were optimized at the M06-2X [34] in conjunction with the 6-311++G (d) level basis set. Polarized continuum models (PCM) were used to investigate the bulk solvent (dielectric constant:78.5) effect.

The interaction energies (E_i) were defined according to the following equation:

$$E_i=E(CH_2=CHOH\cdots C_6H_{12}O_6)-E(C_6H_{12}O_6)-E(CH_2=CHOH) \quad (1)$$

where $E(C_6H_{12}O_6)$, $E(CH_2=CHOH)$, and $E[CH_2=CHOH\cdots C_6H_{12}O_6]$, are the total energies with the counterpoise (CP)[35,36] correction for the isolated $C_6H_{12}O_6$ molecule, the $CH_2=CHOH$, and the corresponding $CH_2=CHOH\cdots C_6H_{12}O_6$, respectively, to eliminate the basis-set superposition error (BSSE). Oxyen atom charges are calculated by fitting the molecular electrostatic potential (CHELPG method).[37]

3. Results and Discussion

3.1 Hydrophilicity of PVA

The hydrophilicity of the anode for MFC is necessary for the formation of a biofilm, which is related to that of binder used in the anode. The hydrophilicity of a binder is related to its molecular structure. The molecular structure of PVA was compared with PTFE by Fourier transform infrared spectroscopy. In the FTIR spectrum of PVA, as shown in Fig. 2A, the broad band at 3362 cm^{-1} is corresponding to hydrogen bonding, the strong band at 1569 cm^{-1} and the broad band at 633 cm^{-1} are corresponding to the stretching vibration and the bending vibration O-H, respectively, which are characteristic of PVA.[38] The peak at 1089 cm^{-1} is attributed to the C-O of C-O-H stretch vibration. The spikes at 2926 cm^{-1} and 1434 cm^{-1} are assigned to the stretching and bending vibration of alkyl C-H, respectively.[39] The strong peak at 1569 cm^{-1} is due to the C=C stretch vibration. Small peak at 842 cm^{-1} can be assigned to C=C stretching of $RCH=CH_2$ in the tail of PVA. For the PTFE (Fig. 2B), the spectrum is smooth from 3000 and 3600 cm^{-1}, illustrating that PTFE does not have any oxygen-containing groups. The spikes at 1233-1157 cm^{-1} and 633 cm^{-1}, 504 cm^{-1} are assigned to the stretching and bending vibration of C-F, respectively.

The different molecular structure might lead to the different thermal stability of PVA and PTFE. Fig. 2C and D presents the TG curves of PVA, PTFE, PVA/CNT and PTFE/CNT under air atmosphere from

room temperature to 750 °C at a heating rate of 10 °C min^{-1}. It can be found from Fig. 2C that PVA experiences a thermal degradation at two stages. The first stage is at about 247-366 °C, which can be ascribed to the condensation reaction of hydroxide radical groups, the second one is at about 366-500 °C, which is attributed to the decomposition of the polymer backbone.[40-42] The small weight loss before 247 °C can be ascribed to the adsorbed water in sample. As shown in Fig. 2D, PTFE begins to decompose at 476 °C, indicating that PTFE has better thermal stability than PVA. Nevertheless, PVA is stable at the temperature lower than 247 °C, which is high enough for binder use in anode of MFC where the temperature is not over 100 °C. When CNTs are introduced, similar weight loss behavior can be observed (Fig. 2C and D), indicating that the thermal stability of both binders is hardly affected by CNTs. As shown in Fig. 2C and D, the weights in all the samples finally decrease to almost zero, suggesting that the carbon backbone of PVA, PTFE and CNTs disappears and PVA, PTFE and CNTs can be burnt completely under air atmosphere at high temperature.

The hydrophilicity of PVA and PTFE was compared by measuring the contact angle. Fig. 2E shows the contact angle on PTFE/CNTs and PVA/CNTs films. 10 μL deionized water was dropped on the resulting films and the morphology of the water droplet was observed. The contact angle for PVA/CNTs (22.2°) is far smaller than that for PTFE/CNTs (95°). Similar phenomenon can be observed on the films without CNTs, as shown in Fig. S3. This comparison indicates that PVA has far better hydrophilicity than PTFE, which should be related to the presence of the oxygen-containing groups in PVA.

3.2 Interaction of PVA with bacteria

Besides the hydrophilicity, the anode should combine bacteria friendly for the formation of biofilm. This nature is related to the interaction between electrocatalyst or binder and bacteria. The interaction of PVA with bacteria was compared with PTFE by theoretical calculations. As shown in Fig. 3A, lipid polysaccharide (LPS) is the main component of the outer membrane in *E. coli*, which consists of an O-antigen polymer (the outermost part), a core oligosaccharide and lipid A.[43] The O-polysaccharide is an unbranched linear polymer of repeating pentasaccharide unit (3-7), which is composed of D-glucose, D-galactose and their single-substitutions, 2/3-acetamido-glucose/galactose. [44-46] To calculate the interaction between binder and bacteria, the binders, PVA and PTFE, and the outer membrane of *E. coli* are simplified as vinyl alcohol (VA), tetrafluoroethylene (TFE) and D-glucose, respectively. The optimized structures of these simplified units before and after their interaction are shown in Fig. 3B. The calculated hydrogen bond length and interaction energy are presented in Table S1. It can be seen from Fig. 3B and Table S1 that there is hydrogen-bond interaction between VA and D-glucose and the smallest hydrogen bond length between VA and D-glucose is 1.78 Å. On the other hand, the calculated interaction energy between VA and D-glucose is -48.43 KJ/mol, more negative than that of TFE (-18.09 KJ/mol), indicating that PVA has stronger interaction with bacteria than PTFE.

To compare the interaction between PVA and the glucose in O-polysaccharide with the glucose in the electrolyte, the optimized structures and oxygen atom charges of simple glucose and O-polysaccharide are calculated. The obtained results are presented in Fig. S4 and the charges of the representative oxygen atoms are listed in Table S2. It can be seen from Table S2 that the oxygen atom charge of glucose in O-polysaccharide is more negative than that in simple glucose, suggesting that O-polysaccharide (bacteria) has stronger interaction with PVA than the glucose in electrolyte. In other words, PVA facilitates the formation of biofilm rather than the adsorption of the glucose from electrolyte.

It is obvious that substituting PVA for PTFE increases the hydrophilicity of anode electrocatalyst (CNTs) and facilitates the formation of biofilm. These effects should promote the electron transfer between bacteria and CNTs thus enhances the power output of MFC.

3.3 Performance of MFCs

To evaluate the effect of the binders on the

performance of MFC, cube MFC (Fig. S2) was constructed with CNTs as anode electrocatalyst and the cell performance was monitored under the same conditions. Fig. 4 presents the power outputs of the MFCs using different binders, obtained by linear sweep voltammetry. It can be seen from Fig. 4 that the cell using 10% PVA yields its maximum power output of 1.631 $W \cdot m^{-2}$. This value is 97.9% greater than that using 5% PTFE, 0.824 $W \cdot m^{-2}$, which is the largest one of the cell using different content of PTFE, as evaluated in Table 1. When the MFCs were test by constant resistance, similar results were obtained, as shown in Fig. S5. This comparison indicates that the power output of the MFC can be improved significantly by substituting PVA for PTFE as binder of anode electrocatalyst. This improvement should be attributed to the better hydrophilicity of PVA and the stronger interaction of PVA with bacteria than PTFE, as demonstrated by the contact angle test and the theoretical calculation.

To evaluate the effectiveness of PVA on the MFC based on other bacteria, the performances of MFCs inoculated with supernatant of an acclimated sludge from a methane-generating pond were also determined. The obtained results are presented in Fig. S6. The maximum power output of cells using PVA is 1.385 $W \cdot m^{-2}$, higher than that using PTFE (0.877 $W \cdot m^{-2}$). This evaluation indicates that the PVA on anode is also suitable for other bacteria.

It can be noted from Fig. 4 that power output of the PVA-based MFC is related to the contents of PVA in anode. The MFC using 10% PVA has the largest maximum output power, but increasing or decreasing the content of PVA reduces the maximum power output. There is a decrease of 51.4% and 36.7% in the maximum power output for the cell using 5% and 15% PVA, respectively.

The effect of PVA content can also be identified by chronoamperometry. Fig. 5 presents the current responses of MFCs freshly inoculated with the *E. coli* cell suspension using 2 $g \cdot L^{-1}$ glucose as substrate under constant voltage (0.1V vs. Ag/AgCl). It can be seen from Fig. 5 that the current increases quickly during the initial inoculation, which reflects the formation process of a biofilm through the bacteria growing or adhering onto anode; reaches a maximum at a certain time, which represents the electron transfer on the anode with the maximum amount of bacteria; and then decreases, which results from exhaustion of glucose.[22,47] The maximum current is 53 mA for the cell using 10% PVA, larger than those using 5% and 15% PVA (27 mA and 38 mA, respectively). This effect can be explained by the balance between the positive contribution in hydrophilicity and interaction with bacteria and the negative one in electronic insulation of PVA. The electron transfer between anode and bacteria requires not only the contact between anode and bacteria vis biofilm but also electronic conductivity of the anode. Using PVA as the binder, the anode facilitates the formation of the biofilm and exhibits the improved electron transfer kinetics. However, the electron transfer kinetics will be retarded when the content of PVA is too high due to its electronic insulation (as showed in Fig. $1A_2$ and $1B_2$).

To confirm the effect of PVA on the electron transfer kinetics between anode and bacteria, electrochemical impedance spectroscopy (EIS) were performed on the MFCs after inoculation with *E. coli* at different time. The obtained results are presented in Fig. 6A-C, which are characteristic of a semicircle at high frequencies and a straight line at low frequencies. The diameter of the semicircle represents the charge transfer resistance (R_{ct}) between the electrode and electrolyte, while the slope of the straight line is assigned to Warburg diffusion.[48-50] On the anode in MFC, R_{ct} reflects the electron transfer between anode and bacteria and can be obtained by fitting. The fitting results are presented in Fig. 6D. It can be found that the R_{ct} of all the cells decreases with the inoculation time, which should be related to the formation process of the biofilm. Among three cells, the cell using 10% PVA exhibits the smallest R_{ct}, indicative of the positive and negative contributions of PVA as binder to the electron transfer kinetics between anode and bacteria.

It should be noted from Fig. 6 A-C that the different contents of PVA has significant influence

upon the diffusion behavior of MFC. This difference should be ascribed to different diffusion model on the anodes with different contents of PVA. Fig. 7 presents the SEM images of the anodes with different contents of PVA after inoculation. The bacteria are scarcely distributed on the surface of the anode with 5% PVA (Fig. 7A), but are heavily aggregated on that of the anodes with 10% (Fig. 7B) and 15% (Fig. 7C) PVA, indicating that increasing the content of PVA facilitates the formation of biofilm on anode. The diffusion limiting reaction process takes place in the solution for the anode with 5% PVA, but does in the biofilm for the anodes with 10% and 15% PVA, leading to the different Warburg impedance behavior (Fig. 6A-C). The anode with 15% PVA does not yield larger power output than that with 10% PVA, confirming that there is a negative contribution of PVA to the electron transfer kinetics between anode and bacteria when its content is too high.

The results above demonstrate that hydrophilic binder in anode plays an important role for the power output of MFCs. This is also true in the case of cathode, as the reported by Hickner and coworkers, who used poly(styrene)-b-poly (ethylene oxide) (PS-b-PEO) and poly(bisphenol A-co-epichlorohydrin) (BAEH) as binders for cathodes to improve the performance of MFC.[51] It can be expected that the power output of MFC can be further improved by using binders with better hydrophilicity.

4. Conclusions

PVA is proposed as an alternative to PTFE as binder for anodic electrocatalyst of MFC. The power output can be improved significantly, almost doubled by substituting PVA for PTFE in an *E. coli*-based MFC using CNTs as anodic electrocatalyst. This improvement is attributed to the better hydrophilicity and stronger interaction of PVA with bacteria than PTFE. However, higher content of PVA might yield negative effect on the electron transfer between anode and bacteria due to its electron insulation. We believe that PVA is also suitable for other MFCs using various anodic electrocatalysts and bacteria.

Acknowledgments

The authors are highly grateful for the financial support from National Natural Science Foundation of China (Grant no. 51471073), Joint Project of Guangdong Province and Ministry of Education for the Cooperation among Industries, Universities and Institutes (Grant no. 2012B090400040) and the scientific research project of Department of Education of Guangdong Province (Grant No.2013CXZDA013).

Notes and References

[a] *School of Chemistry and Environment, South China Normal University, Guangzhou 510006, China*

[b] *Engineering Research Center of MTEES (Ministry of Education), Research Center of BMET (Guangdong Province), Engineering Lab. of OFMHEB (Guangdong Province), Key Lab. of ETESPG (GHEI), and Innovative Platform for ITBMD (Guangzhou Municipality),South China Normal University, Guangzhou 510006, China.*

[c] *Research Resources Center, South China Normal University, Guangzhou 510006, China*

Tel: +8620 39310256; E-mail: liwsh@scnu.edu.cn

1 L. Z. Zeng, L. X. Zhang, W. S. Li, S. F. Zhao, J.F. Lei, Z.H. Zhou, Biosensors & bioelectronics, 2010, 25, 2696-2700.

2 X. Xie, L.B. Hu, M. Pasta, G. F. Wells, D. S. Kong, C. S. Criddle, Y. Cui, Nano letters, 2011, 11, 291-296.

3 R. A. Bullen, T. C. Aront, J. B. Lakeman, F. C. Walsh, Biosensors & bioelectronics, 2006, 21, 2015-2045.

4 B. E. Logan, J. M. Regan, Environmental Science & Technology, 2006, 40, 5172-5180.

5 A. Mekawy, H. Hegab, X. Dominguez-Benetton, D. Pant, Bioresource Technology, 2013, 142, 672-682.

6 Y. Q. Wang, B. Li, L. Z. Zeng, D. Cui, X. D. Xiang, W. S. Li, Biosensors & bioelectronics, 2013, 41, 582-588.

7 Y. Q. Wang, B. Li, D. Cui, X. D. Xiang, W. S. Li, Biosensors & bioelectronics, 2014, 51, 349-355.

8 B. E. Logan, B. Hamelers, R. Rozendal, U. Schröder, J. Keller, S. Freguia, P. Aelterman, W. Verstraete, K. Rabaey, Environmental Science & Technology, 2006, 40, 5181-5192.

9 M. H. Osman, A. A. Shah, F. C. Walsh, Biosensors & Bioelectronics, 2010, 26, 953-963.

10 U. Schröder, Physical chemistry chemical physics : PCCP, 2007, 9, 2619-2629.

11 S. K. Chaudhuri, D. R. Lovely, Nature biotechnology, 2003, 21, 1229-1232.

12 Y. Qiao, S. J. Bao, C. M. Li, X. Q. Cui, Z.S. Lu, J. Guo, ACS Nano, 2007, 2, 113-119.

13 Y. Yuan, J. Ahmed, L. Zhou, B. Zhao, S. Kim, Biosensors & bioelectronics, 2011, 27, 106-112.

14 P. Liang, H. Wang, X. Xia, X. Huang, Y. Mo, X. Cao, M. Fan, Biosensors & bioelectronics,2011, 26, 3000-3004.

15 A. Mehdiniaa, E. Ziaei, A. Jabbari, Electrochimica Acta, 2014, 130, 512-518.

16 E. Li, X. Wang, X. Wang, H. Wang, Advanced Materials Research Vols, 2012, 535-537,149-153.

17 K. Sheng, H. Bai, Y. Sun, C. Li, G. Shi, Polymer, 2011, 52, 5567-5572.

18 M. Amrithesh, S. Aravind, S. Jayalekshmi, R.S. Jayasree, Journal of Alloys and Compounds, 2008, 458, 532-535.

19 Y. Wei, Y. Li, X. Liu, Y. Xian, G. Shi, L. Jin, Biosensors & bioelectronics, 2010, 26, 275-278.

20 L. Z. Zeng, S. F. Zhao., Y. Q. Wang, H. Li, W. S. Li, Int J Hydrogen Energy,2012, 37, 4590-4596.

21 D. Cui, Y. Q. Wang, L. D. Xing, W. S. Li, International Journal of Hydrogen Energy, 2014, 39, 15081-15087.

22 X. F. Chen, D. Cui, X. J. Wang, X. S. Wang, W.S. Li, Biosensors & bioelectronics, 2015, 69, 135-141.

23 Y. Q. Wang, H. X. Huang, B. Li, W. S. Li, J. Mater. Chem. A, 2015, 3, 5110-5118.

24 S. Litster, G. McLean, Journal of Power Sources, 2004, 130, 61-76.

25 T. Zhang, Y. Zeng, S. Chen, X. Ai, H. Yang, Electrochemistry Communications, 2007, 9, 349-353.

26 J. L. Drury, D. J. Mooney, Biomaterials,2003, 24, 4337-4351.

27 M. C. Gutiérrez, Z. Y. García-Carvajal, M. Jobbágy, F. Rubio, L. Yuste, F. Rojo, M. L. Ferrer, F. del Monte, Advanced Functional Materials, 2007, 17, 3505-3513.

28 M. C. Gutiérrez, Z. Y. García-Carvajal, M. Jobbágy, L. Yuste, F. Rojo, C. Abrusci, F. Catalina, F. d. Monte, M. L. Ferrer, Chemistry Materials, 2007, 19, 1968-1973.

29 M. C. Gutiérrez, Z. Y. García-Carvajal, M. J. Hortigüela, L. Yuste, F. Rojo, M.L. Ferrer, F.d. Monte, Journal of Materials Chemistry, 2007, 17, 2992–2995.

30 D. K. Sharma, F. T. Li, Y. N. Wu, Colloids and Surfaces A: Physicochem. Eng. Aspects, 2014, 457, 236–243.

31 J. M. Yang, S. A. Wang, C. L. Sun, M. D. Ger, Journal of Power Sources, 2014, 254, 298-305.

32 L. X. Zhang, C. S. Liu, L. Zhuang, W. S. Li, S. G. Zhou, J. T. Zhang, Biosensors & bioelectronics, 2009, 24, 2825-2829.

33 M. J. Frisch, G. W. Trucks, H. B. Schlegel, G. E. Scuseria, M. A. Robb, J. R. Cheeseman, G. Scalmani, V. Barone, B. Mennucci, G.A. Petersson, Gaussian 09, Revision A, Gaussian, Inc., Wallingford, CT, 2009.

34 L. D. Xing, C. Y. Wang, W. S. Li, M. Q. Xu, X. L. Meng, S. F. Zhao, Journal of Physical Chemistry B, 2009, 113, 5181.

35 S. F. Boys, F. Bernardi, molecular physics, 1970, 19, 553-566.

36 P. Hobza, Z. Havlas, Theoretical Chemistry Accounts, 1998, 99, 372-377.

37 L. D. Xing and O. Borodin, Phys. Chem. Chem. Phys., 2012, 14, 12838-12843.

38 D. S. Kim, M. D. Guiver, S. Y. Nam, T. I. Yun, M. Y. Seo, S. J. Kim, H. S. Hwang, J. W. Rhim, Journal of Membrane Science, 20063, 281, 156-162.

39 S. Mollá, V. Compañ, E. Gimenez, A. Blazquez, I. Urdanpilleta, International Journal of Hydrogen Energy, 2011, 36, 9886-9895.

40 M. Zhou, L. Liu, Z.H. Yang, S. Mao, Y. Zhou, T. T. Hu, Y. Yang, B. W. Shen, X. Y. Wang, Journal of Power Sources, 2013, 234, 292-301.

41 A. Anis, A. K. Banthia, S. Bandyopadhyay, Journal of Power Sources, 2008, 179, 69-80.

42 M. Helen, B. Viswanathan, S. S. Murthy, Journal of Power Sources, 2006, 163, 433-439.

43 C. R. Raetz, annual review of biochemistry,1990, 59, 129-170.

44 A. K. Datta, S. Basu , N. Roy, Carbohydrate Research, 1999, 322, 219-227.

45 M. B. Perry, L. L. MacLean, Carbohydrate Research, 1999, 322, 57-66.

46 L. L. MacLean, Y. H. Liu, E. Vinogradov, M. B. Perry, Carbohydrate Research, 2010, 345, 2664-2669.

47 L. X. Zhang, S. G. Zhou, L. Zhuang, W. S. Li, J. T. Zhang, N. Lu, L. F. Deng, Electrochemistry Communications, 2008, 10, 1641-1643.

48 Z. Z. Qiu, M. Sun, L. L. Wei, H. L. Han, Q. B. Jia, J. Q. Shen, Journal of Power Sources, 2015, 273, 566-573.

49 X. L. Liao, Q. M. Huang, S. W. Mai, X. S. Wang, M. Q. Xu, L. D. Xing, Y. H. Liao, W. S. Li, Journal of Power Sources, 2014, 272, 501-507.

50 D. S. Lu, W. S. Li, X. X. Zuo, Z. Z. Yuan, Q. M. Huang, Journal of Physical Chemistry C, 2007, 111, 12067-12074.

51 T. Saito, T. H. Roberts, T. E. Long, B. E. Logan, M. A. Hickner, Energy & Environmental Science, 2011, 4, 928-934.

Figure and Table Captions

Fig. 1. Schematic electron transfer mechanism between bacteria and anode of MFC (direct contact with CNT (A_1) and binder (A_2) via microbial wall and long-range electron transfer with CNT (B_1) and binder (B_2) via microbial nanowires). .

Fig. 2. FTIR spectra (A, B), TG curves (C, D) and contact angles (E) of water droplets on binder/CNT films.

Fig. 3. Schematic bacterium membrane (A) and the optimized structures (B) of simplified PVA, PTFE and outer membrane of *E. coli* before and after their interaction.

Fig. 4. Power outputs of cube MFCs with different binders, obtained by linear sweep voltammetry.

Fig. 5. Current responses of MFCs with different contents of PVA. The cells were freshly inoculated with the *E. coli* cell suspension using 2 $g \cdot L^{-1}$ glucose as substrate under constant voltage (0.1V vs. Ag/AgCl).

Fig. 6. Electrochemical impedance spectra of MFCs with different contents of PVA in the solution containing 2 g/L glucose after inoculation with *E. coli* for 20 hr (A), 45 hr (B) and 70 hr (C), and variation of charge transfer resistance (D) on anode of MFCs with different contents of PVA (The inset is the equivalent circuit).

Fig. 7. SEM images of the electrodes with different contents of PVA: 5% (A), 10% (B) and 15% (C).

Table 1 Parameters of MFC using different binders

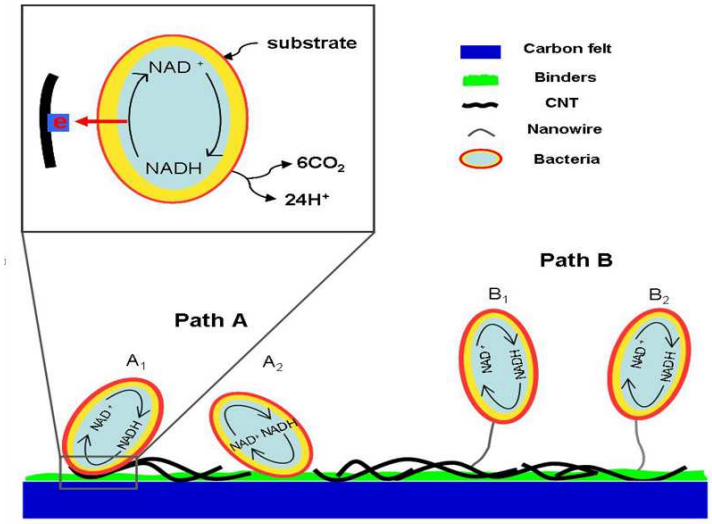

Fig. 1. Schematic electron transfer mechanism between bacteria and anode of MFC (direct contact with CNT (A_1) and binder (A_2) via microbial wall and long-range electron transfer with CNT (B_1) and binder (B_2) via microbial nanowires).

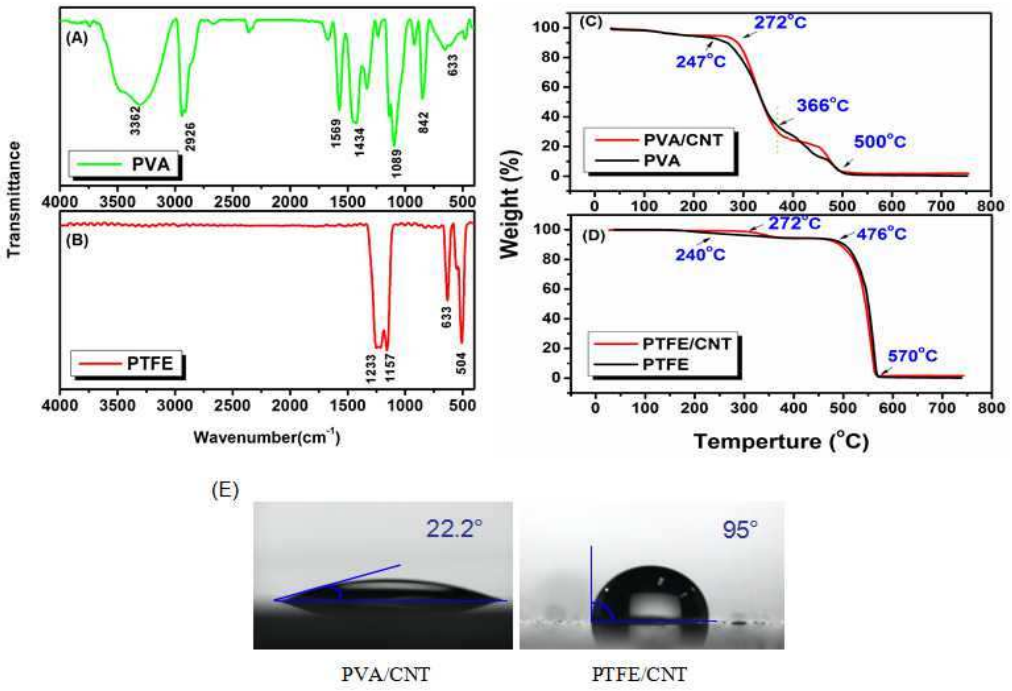

Fig. 2. FTIR spectra (A, B), TG curves (C, D) and contact angles (E) of water droplets on binder/CNT films.

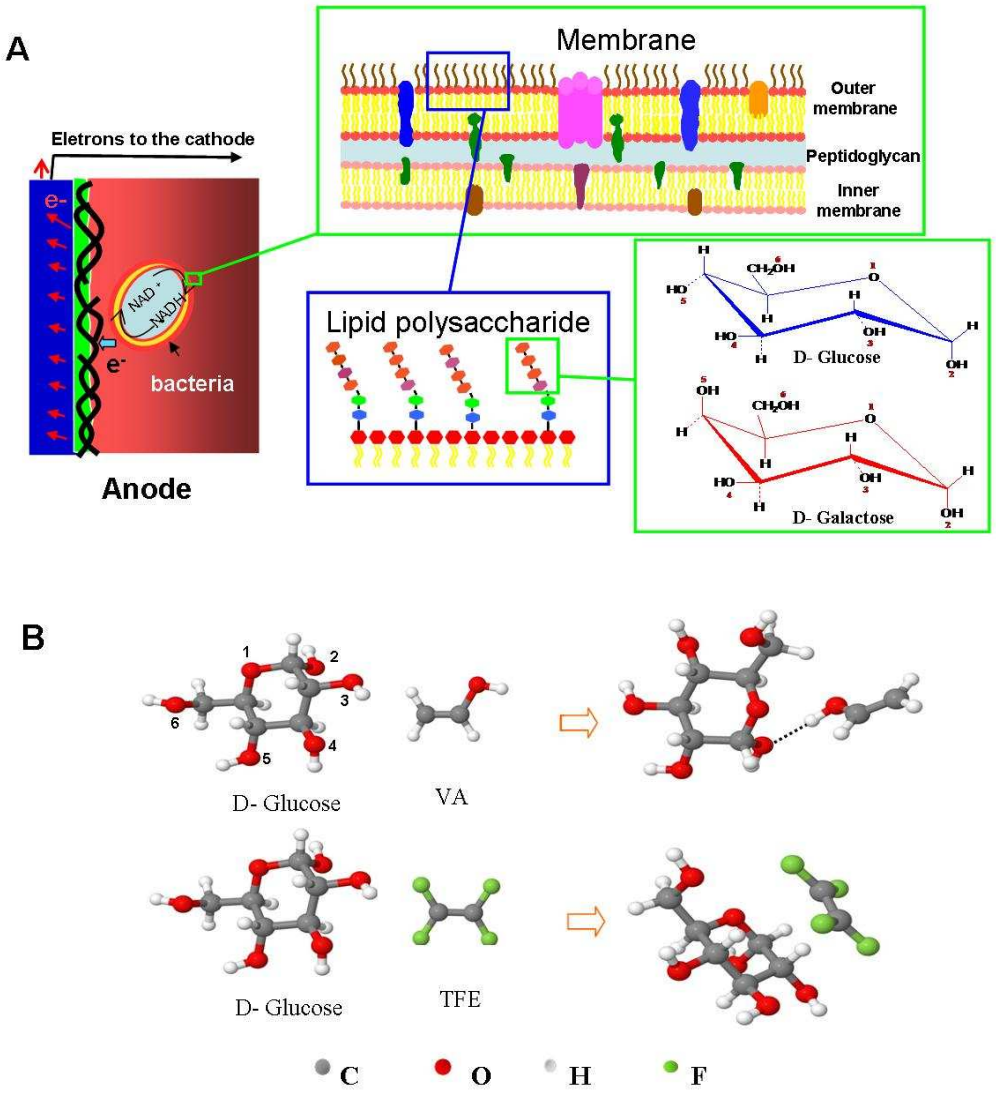

Fig. 3. Schematic bacterium membrane (A) and optimized structures (B) of simplified PVA, PTFE and outer membrane of *E. coli* before and after their interaction.

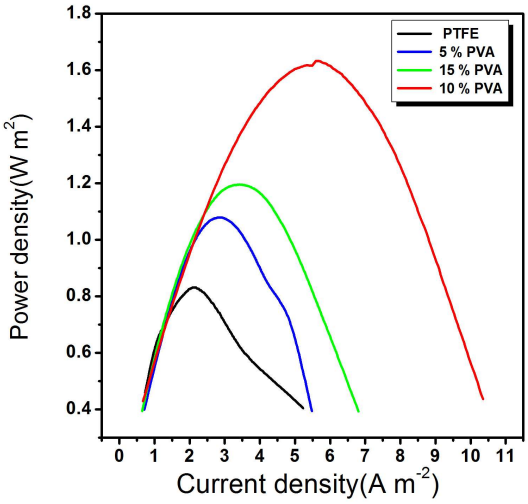

Fig. 4. Power outputs of cube MFCs with different binders, obtained by linear sweep voltammetry.

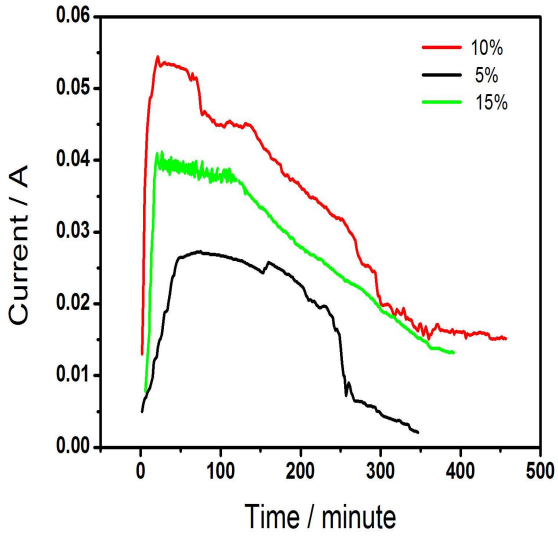

Fig. 5. Current responses of MFCs with different contents of PVA. The cells were freshly inoculated with the *E. coli* cell suspension using 2 $g \cdot L^{-1}$ glucose as substrate under constant voltage (0.1V vs. Ag/AgCl).

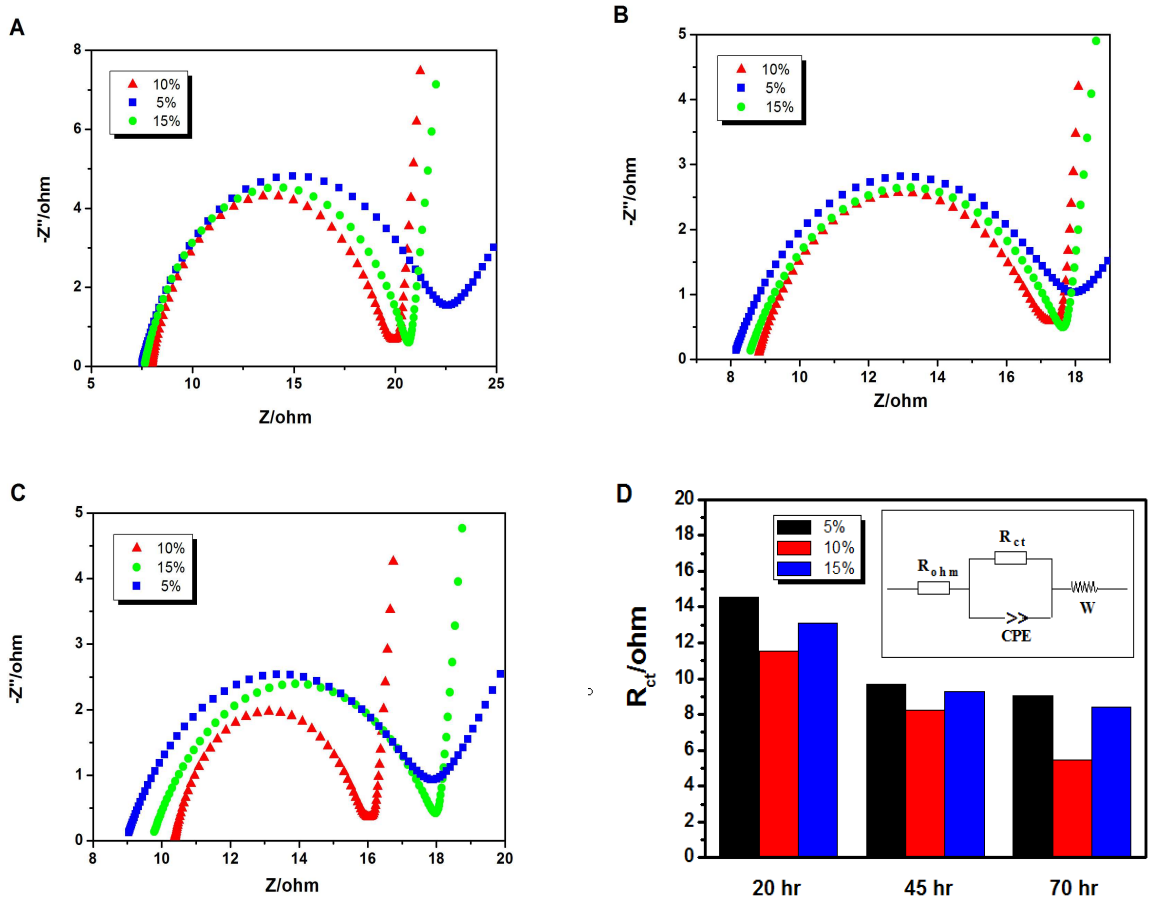

Fig. 6. Electrochemical impedance spectra of MFCs with different contents of PVA in the solution containing 2 g/L glucose after inoculation with *E. coli* for 20 hr (A), 45 hr (B) and 70 hr (C), and variation of charge transfer resistance (D) on anode of MFCs with different contents of PVA (The inset is the equivalent circuit).

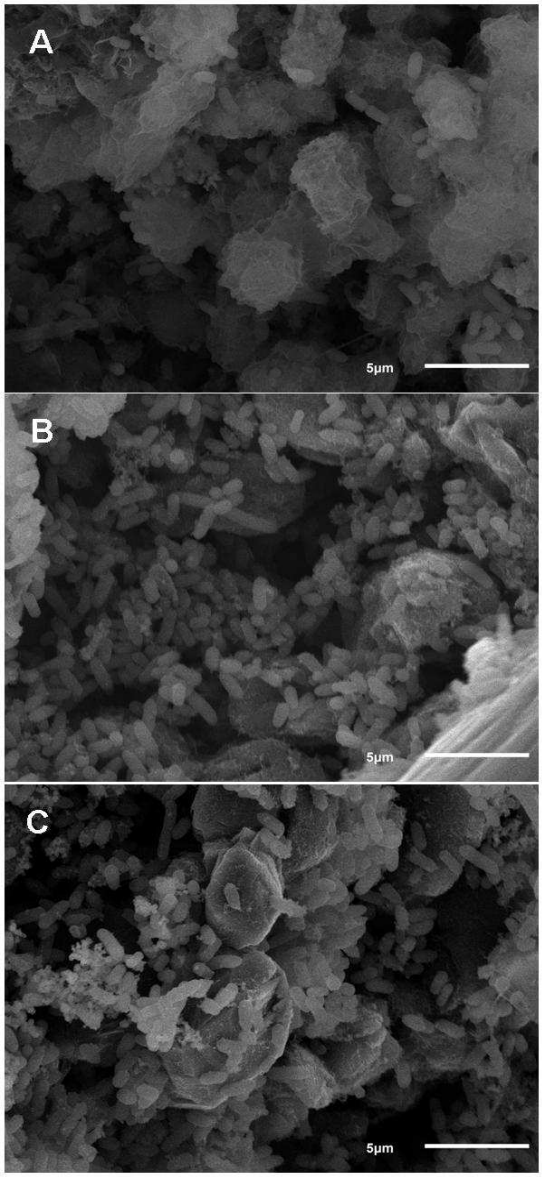

Fig. 7. SEM images of the electrodes with different contents of PVA: 5% (A), 10% (B) and 15% (D).

Table 1 Parameters of MFC using different binders

Binder	Internal resistance (Ω)	Maximum power density ($W \cdot m^{-2}$)	Maximum current density ($A \cdot m^{-2}$)
1%PTFE	229	0.648	1.68
5%PTFE	214	0.824	2.07
10%PTFE	220	0.742	1.84
5%PVA	138	1.077	2.79
10%PVA	54	1.631	5. 50
15%PVA	100	1.193	3.45